(12)

ADVANCED ARTIFICIAL DIELECTRIC MATERIALS FOR MILLIMETER WAVELENGTH APPLICATIONS

Annual Technical Report, Part A

Contract No. N00014-83-C-0447

ISRAEL S. JACOBS

General Electric Company
Corporate Research and Development
P.O. Box 8
Schenectady, New York 12301

Report Period 1 Oct 1984 - 30 Sept 1985

Prepared for

Office of Naval Reseach
800 North Quincy Street
Arlington, Virginia 22217

85-SRD-030

UNCLASSIFIED

SECURITY CLASSIFICATION OF THIS PAGE

REPORT DOCUMENTATION PAGE

1a. REPORT SECURITY CLASSIFICATION UNCLASSIFIED	1b. RESTRICTIVE MARKINGS
2a. SECURITY CLASSIFICATION AUTHORITY	3. DISTRIBUTION/AVAILABILITY OF REPORT Reproduction in whole or in part is permitted for any purpose by the United States Government
2b. DECLASSIFICATION/DOWNGRADING SCHEDULE	
4. PERFORMING ORGANIZATION REPORT NUMBER(S) 85-SRD-030	5. MONITORING ORGANIZATION REPORT NUMBER(S)
6a. NAME OF PERFORMING ORGANIZATION General Electric Company Corporate Research and Development 6b. OFFICE SYMBOL *(If applicable)*	7a. NAME OF MONITORING ORGANIZATION Office of Naval Research Code 431
6c. ADDRESS *(City, State and ZIP Code)* P.O. Box 8 Schenectady, NY 12301	7b. ADDRESS *(City, State and ZIP Code)* 800 North Quincy Street Arlington, VA 22217
8a. NAME OF FUNDING/SPONSORING ORGANIZATION 8b. OFFICE SYMBOL *(If applicable)*	9. PROCUREMENT INSTRUMENT IDENTIFICATION NUMBER N00014-83-C-0447
8c. ADDRESS *(City, State and ZIP Code)*	10. SOURCE OF FUNDING NOS. PROGRAM ELEMENT NO. 61153N; PROJECT NO. RR02202; TASK NO. OC; WORK UNIT NO.
11. TITLE *(Include Security Classification)* ADVANCED ARTIFICIAL DIELECTRIC MATERIALS (U)	
12. PERSONAL AUTHOR(S) I.S. Jacobs	
13a. TYPE OF REPORT Annual Report	13b. TIME COVERED FROM 84 Oct 01 TO 85 Sept 30
14. DATE OF REPORT *(Yr., Mo., Day)* 85 Dec 30	15. PAGE COUNT 34
16. SUPPLEMENTARY NOTATION Full title of contract: Advanced Artificial Dielectric Materials for Millimeter Wavelength Applications (U)	

17. COSATI CODES		
FIELD	GROUP	SUB. GR.

18. SUBJECT TERMS *(Continue on reverse if necessary and identify by block number)*
Artificial dielectrics, properties of heterogeneous media
fine powder preparation and characterization, permittivity
and induced permeability

19. ABSTRACT *(Continue on reverse if necessary and identify by block number)*

This is Part A of a two-part Annual Report. (Part B, dealing with magneto-dielectrics, is classified.) This part describes a continuation of work on artificial dielectric composites based on a polymeric binder and alloy powder particles that are oxide-coated for isolation and ferromagnetic below room temperature for packing determination. Characterization studies show the surface oxide on the alloy powder. Microstructural study of the composites shows wide variations in local packing density, characteristic of random loading. Permittivity measurements extended to 35 GHz correlate qualitatively with modern theories of heterogeneous media but evidence deviations that may arise from the observed clumping. Higher frequency measurements of permittivity and induced permeability are under way. An alternative inorganic binder material and process (with higher dielectric constant) has been developed with properties suitable for the morphological, electromagnetic, and mechanical requirements.

20. DISTRIBUTION/AVAILABILITY OF ABSTRACT UNCLASSIFIED/UNLIMITED ☐ SAME AS RPT. ☒ OTIC USERS ☐	21. ABSTRACT SECURITY CLASSIFICATION UNCLASSIFIED
22a. NAME OF RESPONSIBLE INDIVIDUAL Dr. D.E. Polk (ONR)	22b. TELEPHONE NUMBER (202) 696-4401 22c. OFFICE SYMBOL Code 431M

DD FORM 1473, 83 APR EDITION OF 1 JAN 73 IS OBSOLETE.

UNCLASSIFIED

SECURITY CLASSIFICATION OF THIS PAGE

TABLE OF CONTENTS

LIST OF ILLUSTRATIONS

LIST OF TABLES

PREFACE

This report was prepared by General Electric Corporate Research and Development under ONR Contract No. N00014-83-C-0447. The Principal Investigator was Dr. Israel S. Jacobs of the Electronic Materials and Devices Unit, VLSI Technology Laboratory.

The program was administered under the direction of CDR William R. Schmidt, USN, Code 430B, of the Office of Naval Research, Arlington, VA, 22217. At the end of this reporting period, however, the responsibility for administration was transferred to Dr. Donald E. Polk, Code 431M, of ONR.

SUMMARY

This program is concerned with the development of a novel class of artificial dielectrics and a deeper understanding of its properties and millimeter wavelengths. The work is divided between two subclasses, one of essentially nonmagnetic composite dielectrics and one of composite magneto-dielectrics. Inasmuch as some aspects of the latter group are classified, this annual report appears in two sections, Parts A and B. This portion is Part A; the magneto-dielectric work appears in a subsequent classified section, Part B.

In this second year of the program, study continued on artificial dielectric composites based on a polymeric binder and the alloy powder of $Ni_{92}Cr_8$, prepared by gas-water atomization to be oxide-coated for isolation and ferromagnetic *below* room temperature for packing determination. An improved characterization of the surface condition of the alloy powder particles demonstrated the presence of an insulating oxide. Microstructural study of the polymeric composites at various volume loadings shows wide variations in local packing density that are characteristic of random loadings. Electromagnetic measurements on these composites were extended to about 18 GHz in the centimeter wavelength range, and to a fixed point at 35 GHz at the entry to the millimeter range. Additional powder and samples were prepared for measurements (being performed at the Naval Research Laboratory) in the millimeter range. Measurements of permittivity versus volume loading at 35 GHz conform generally to the prediction of modern calculation both in a (classical) smooth departure from the host binder value and in an upward deviation from the classical Clausius-Mossotti/Maxwell calculation. This improves our prior evidence for higher-order multipole effects in random systems. However, the upward deviation with volume loading is steeper than predicted, which may be a consequence of clumping, i.e., the observed fluctuations in local packing.

To investigate binder permittivity effects, work has proceeded toward developing an alternative inorganic binder with a higher dielectric constant. After experimenting with various glasses and processing steps, a suitable candidate has been found that appears to meet the requirements of retaining alloy particle shape, alloy chemical integrity, electrical isolation, and mechanical integrity for machinability.

I. INTRODUCTION

This research is concerned with the development of a novel class of artificial dielectrics and a deeper understanding of its properties at millimeter wavelengths. This is the second year of the program. Our original point of departure was the Theoretical Radar Absorbing Materials Physics Model developed during a classified program [1]. That study involved experiment and analysis of a broad data base obtained from measurements in the microwave range of frequencies (centimeter wavelengths). However, many of the model features and predictions are relevant to the millimeter wavelength region. From the outset, the present work was divided between two subclasses, one of essentially nonmagnetic composite dielectrics and one of composite magneto-dielectrics. Some aspects of work on the magneto-dielectrics are classified. Therefore, this annual report is prepared in two sections, Parts A and B, with the magneto-dielectrics work appearing in the subsequent *classified* section, Part B.

We first review briefly the work of the initial year [2]. An artificial dielectric (essentially nonmagnetic) polymeric composite was developed containing metallic alloy particles ($Ni_{92}Cr_8$) that are oxide-coated for isolation and ferromagnetic *below* room temperature to facilitate packing determination. Particle size, resisitivity, and volume loading are significant factors in the electromagnetic properties of such composites. Induced magnetic dipole (eddy current) effects, depending markedly on the ratio of particle radius to skin depth, were perceived to be relevant, and were calculated and found to be in accord with initial measurements of complex permeability in the centimeter wavelength range (6 to 12 GHz). An up-to-date exploration of theoretical descriptions of the dielectric properties of heterogeneous media was made. They accounted for the general features of the relatively simple Maxwell (Maxwell-Garnett, Clausius and Mossotti) behavior observed for artificial dielectrics of the present class. Evidence for higher-order multipole interactions and geometrical packing limits were perceived in the results found in random composites. Additional deviations from prediction suggested a path for future research.

Work was also initiated on alternative passivation coatings and on the preparation of very fine powders by the spark erosion method. Such powders are intended for use in the magneto-dielectric composites.

During this second year of the program a number of co laborators and consultants participated significantly, and many of them would qualify as co-authors if this were a normal publication. We therefore list them here, with their areas of contribution properly attributed: For preparation of alloy powders by gas-atomization and exploration of alternative coatings, S.A. Miller with D.N. Wemple (GE-CRD); for search for alternative (inorganic) binder, M.P. Borom with L.E. Szala (GE-CRD); for experimental research on the spark erosion method, A.E. Berkowitz and J.L. Walter with J.J. Roger and W.E. Rollins (GE-CRD); for a wide range of measurement responsibility for the principal investigator, including thermomagnetic, microwave and Mössbauer spectroscopy, H.J. Patchen (GE-CRD); for microwave measurements at K_α band frequency, J.O. Hansen (GE-Re-Entry Systems Operation, Philadelphia); for preparation of polymeric composites, D.B. Lindeman (GE-Aircraft Engine Group, Cincinnati); for consultation and measurements at millimeter wavelengths, D.W. Forester and F.J. Rachford (Naval Research Laboratory, Washington, D.C.); for consultation on fine particle separation, D.R. Kelland (National Magnet Laboratory, MIT); for general consultations on physics and measurements, Prof. W.P. Wolf (Yale University) and Prof. W.T. Doyle (Dartmouth College).

This unclassified portion of the Annual Report covers work described under Tasks 1 to 3 of the original program schedule. Their titles are as follows: Investigate Effect of

Binder Permittivity in Artificial Dielectrics, Analyze Effects of Microstructure Control in Passivated Metal-Insulator Composites, and Develop Alternative Theoretical Approaches to Composite Dielectrics. An additional task (Task 4) was removed by agreement with the ONR Scientific Officer, in return for expansion of effort under Tasks 1 and 3. The subsequently numbered tasks (Tasks 5 through 8) fall more easily into the classified portion of the report.

II. POLYMERIC BINDER COMPOSITE DIELECTRIC

This section focuses on the essentially nonmagnetic Ni-Cr alloy artificial dielectric prepared with the polyurethane polymeric binder as described previously [2]. Efforts at developing an alternative inorganic binder with higher ϵ' will be described in Section III.

II.1 Extension of Frequency Range of Measurements

In the previous report, we presented results for complex permittivity and permeability for the frequency range 6 to 12 GHz, as obtained with a network analyzer. The same system, augmented by a different frequency sweep generator plug-in, was used to extend the measurements to about 18 GHz during the recent period.

As announced in the prior report, we contracted to obtain measurements at 35 GHz at GE Re-Entry Systems Operation in Philadelphia. The method was based on the slotted-line technique with a circular waveguide cavity. It has the advantage of requiring a small (0.250-inch diameter), thin disk. This is much less demanding of material than that originally requested by NRL for the arch method. It also is easier to fabricate than, for example, the precision coaxial toroid, when the question of machinability arises as it does in Section III. The results from these measurements are presented in Sections II.4 and II.5.

According to the provisions of the contract, millimeter wavelength region measurements for this study are to be performed at the Naval Research Laboratory, Washington, D.C. Toward this goal, a visit was made to NRL in February 1985 for discussions with Dr. D.W. Forester and Dr. F.J. Rachford. It was agreed that measurements would be attempted by several techniques, including the arch method at rather high frequencies (~90 GHz), and waveguide techniques at several high-frequency bands, e.g., K_α (26-40 GHz), Q (40-60 GHz), and W (75-110 GHz). Such a wide range of frequencies, coupled with the particle size effects discussed in the prior report, offers an exciting prospect for testing the induced permeability model as well as for amplifying our understanding of the permittivity behavior. It was necessary to make another powder preparation run to prepare the desired samples. The characterization of the new atomized powder and of the composites prepared therefrom are given in Section II.2. The samples were delivered to NRL early in June 1985, and work is in progress at this writing.

II.2 New Powder and Sample Preparation

Following the choices and methods of the prior report [2], another powder lot (designated RS-98) was made by gas-water atomization from a melt of Ni92Cr8. The prior description neglected to spell out that a blast of water spray follows the gas jets [3] (see Figure 1). This is now believed to contribute to shifting the size distribution toward smaller particles, as well as to promoting the desired surface oxidation of the powder particles.

A thermomagnetic scan of this powder lot is shown in Figure 2, along with those from the earlier work, RS-67, and the two ingot pieces at 8 wt% and 6 wt% Cr. From the mid-range Curie point of 154 K (about 11 K lower than for RS-67) we infer a composition of 7.35 wt% Cr (or ~8.2 at%) using the data of Reference 2. The specific magnetization, ex-

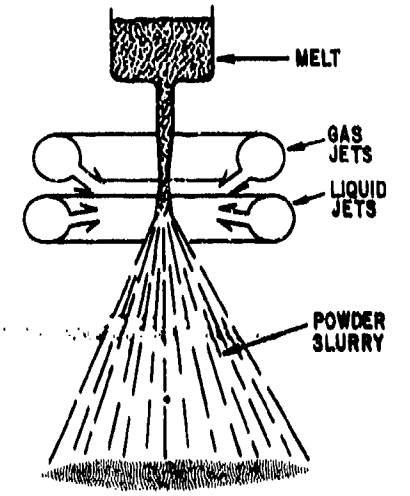

Figure 1. Gas-liquid atomization

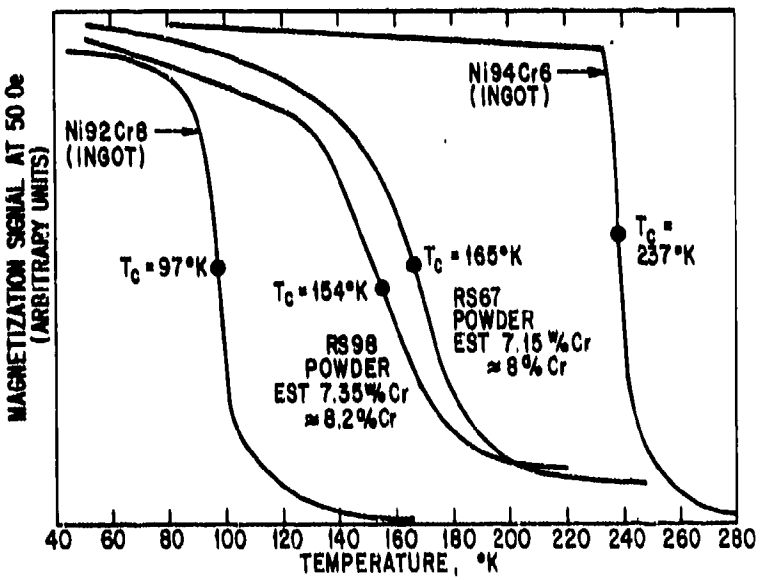

Figure 2. Thermomagnetic analysis of Ni-Cr ingots and atomized powders.

trapolated to high fields, at 6 K, is 14.6 emu/g. The upward shifts from the bulk alloy are in the direction expected for a relative preferential oxidation of Cr over Ni.

The powder that sieved out below 325 mesh (37 μm) was subsequently air-classified into three size fractions: <10 μm, 10 to 20 μm, and >20 μm, at Alpine American Corp. of Natick, Massachusetts. The yields obtained were as follows: 550 g at <10 μm, 185 g between 10 and 20 μm, and 670 g >20 μm.

From the discussions at NRL, it was decided to measure rather highly loaded samples, i.e., volume loading of $p = 0.40$. In order to continue the particle size study commenced in the prior portion, we chose the two extremes, i.e., <10 μm and 20 to 37 μm. Test

coupons of powder (RS-98) with polyurethane binder were prepared according to the techniques of Reference 2, Section II.1.6.2. Two coupons for each particle size were made, one was $4 \times 4 \times 0.045$ inch for preparation of the arch method test piece and the second was about $1 \times 2 \times 0.080$ inch for subsequent precision cutting of waveguide pieces.

The actual volume loadings and estimated porosities were calculated following density measurements of the coupons and low temperature (~6 K) magnetization measurements of smaller pieces cut therefrom. These results are presented in Table 1. The p values are obtained from the formula:

$$p = \frac{\sigma_c \rho_c}{\sigma_a \rho_a},$$

where c and a refer to composite and bare alloy, respectively, σ is the magnetization (low temperature, extrapolated to high field) and ρ is the density of the particular component. Note that coated powder density can be different from that of the bare alloy. The porosity is estimated from a formula derived in Reference 2., i.e.,

$$f_h^v = 1 - \frac{\rho_c}{\rho_b} + \frac{\sigma_c \rho_c}{\sigma_a} \left[\frac{1}{\rho_b} - \frac{1}{\rho_a} \right],$$

where the b subscript refers to the binder. While the p-value formula leads to rather accurate determinations, the formula for porosity, f_h^v, amplifies uncertainties in ρ_b, ρ_c, etc., because of the subtraction of comparable terms.

We see from Table 1 that the larger powder size material coupons came quite close to the goals set ($p = 0.4$) while the $< 10\ \mu$m powder composite coupons fell short.

At millimeter wavelengths, the samples must be cut with high precision. The 3×3-inch plate samples for the arch method were trimmed to thicknesses estimated at

Table 1

DESCRIPTION OF POLYURETHANE TEST COUPONS FOR NRL HIGH-FREQUENCY MEASUREMENT SAMPLES

- Powder from atomization run RS-98 (Alloy 8.2 at% Cr in Ni; T_c = 154 K ±20)
- All intended for nominal 40% volume loading (p = 0.40)
- Two powder particle size ranges chosen

Coupon Slab	Particle Size (μm)	Measured p	Measured Density	Calculated Porosity f_h^v
A Waveguide pieces: K_a, Q, W	< 10 μm	0.36	3.63_4	0.19
B Arch slab	< 10μm	0.27	3.10_0	0.07
C Waveguide pieces: K_a, Q,W	>20-37μm	0.42	4.31_8	0.01
D Arch slab	>20-37μm	0.39	4.04_0	0.08

(3/4) λ_m, where λ_m is the wavelength *in* the medium at W band (90 GHz). Estimates for λ_m were arrived at from modeling of induced μ' behavior as a function of frequency, particle size, alloy resistivity, and volume loading, and from the ϵ' model, assuming no frequency dependence. The models were discussed last year [2]. The formula for the wavelength in the medium is $\lambda_m = \lambda_o/[\epsilon'\mu']^{1/2}$, where λ_o is the vacuum wavelength. Even more demanding are the samples to fit into the waveguides of the separate bands. These have rigid linear tolerances as well as thickness requirements. The desirable thicknesses are again an odd number of quarter-wavelengths. However, for this measurement one refers to the guide wavelength [4], λ_g, given by

$$\lambda_g = \frac{\lambda_m}{[1 - (\lambda_o/\lambda_c)^2]^{1/2}},$$

where λ_c is the cutoff wavelength of the particular waveguide which is a function of the waveguide dimensions [4]. In some cases we could get by with quarter-wavelength pieces. At higher frequencies, these would be so thin as to force a choice to three-quarter-wavelength thicknesses.

II.3 Microstructural Observations

In this section we add to observations reported last year [2] on two levels of microstructure, i.e., on the surface coating of the gas-water atomized powder and on the gross structure of the composite (alloy powder plus binder).

II.3.1 Evaluation of Surface Condition of Metal Powder

The upward shift in Curie temperature from original ingot to atomized powder denotes a greater depletion of Cr from the alloy particle than of Ni. On the other hand, we reported [2] a depth profile by Auger electron spectroscopy from which the surface composition appears to be dominated by oxidized nickel, although some chromium oxide is also suggested. The alloy powder was pressed into a soft metal base and sputtered away slowly. In fact, attempts at a chemical balance showed that even a small amount of Cr oxide in the oxide shell would allow a noticeable shift in the Cr/Ni ratio of the alloy core because the starting ratio was roughly 1/10. Estimates of the coating thickness derived from the mass balance range from about 0.1 μm to about 0.2 μm.

Our associate, M.D. McConnell of the Microchemical and Surface Analysis Unit, Materials Characterization Operation, used an alternative technique. The Ni-Cr alloy particles were copper-coated by electroless plating (by K.P. Zarnoch) for edge retention, and pressed together to develop an apparently continuous copper matrix. This compact could be polished to expose the particle cross section, and then a traversing scan by Auger electron spectroscopy might reveal an edge coating. The results of such a scan at 8000X embracing parts of two spherical particles are shown in Figure 3. Signals for Ni and O are shown, that for Cr being too weak or overlapping with the others. There is a clear build-up of oxygen at the particle edges. Its thickness could approach 0.5 μm but care should be taken with that interpretation without details on the beam spot size.

The present evidence permits us to conclude with confidence that there is an oxide coating on the particles, one which is probably responsible for the high dc electrical resistance measured crudely on compacts of the powder [2]. However, we cannot conclude the exact chemistry or microstructure of the shell itself. Conventional isothermal oxidation studies of Ni-Cr alloys [5] show that the nature of the oxide coating is rather sensitive to the Cr content and to the oxygen partial pressure, as well as to temperature and

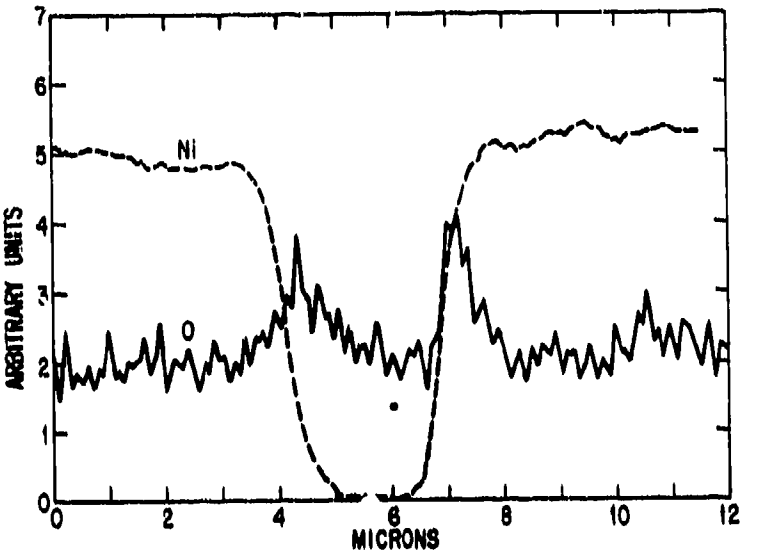

Figure 3. Auger electron spectroscopy microchemical scan for Ni and O across Ni-Cr powder particles ($20 < d < 37\ \mu m$) embedded in copper matrix.

time. At our level of Cr, it seems quite possible that the coating would contain precipitates of Cr_2O_3 in a NiO host, but that is still conjecture [6]. The conditions of temperature and partial pressure of oxygen in the gas-water atomization spray are poorly known.

II.3.2 Observations on Alloy Particle Aggregation in Composites

In the prior report, we presented direct SEM pictures of one composite (ONR No. 2, $p = 0.4$, $20\ \mu m < d < 37\ \mu m$) at low magnifications, 150X and 500X (Figure 26 of Reference 2). Our original purpose was to examine the porosity, which we had calculated to be rather low. That was essentially confirmed. After the fact, we realized that this sort of observation could have importance for the understanding of the dependence of ϵ' on volume loading.

Special equipment was needed, as provided by our associates V.H. Watkins and S.Y. Hobbs of the Polymer Physics Unit. Room temperature microtoming was unsatisfactory because the binder was so soft, but a cold microtoming technique (with the sample at about −150 °C), using a glass knife produced a very satisfactory surface for examination.

We extended the examination during this period to the more dilute samples of the original series (ONR No. 5, $p = 0.1$; ONR No. 4, $p = 0.2$; ONR No. 3, $p = 0.3$; $20\ \mu m < d < 37\ \mu m$, alloy RS-67). This time the microtomed samples were coated lightly with carbon to carry off electrons and heat, instead of with Au and Pd. The result is a much improved visual contrast, as shown in Figure 4, at 150X and 500X. There is clear evidence for spatial fluctuations in local density of alloy particles. As noted in our prior report, fluctuations on some scale could conceivably help to account for some ϵ' versus p behavior. This picture gives a scale to the "clumping." The challenge is whether we can model this in an analytic way. A formal consultation has been negotiated with Professor Doyle of Dartmouth with a view toward tackling this question. The SEM pictures in Figure 4a also show "crevasse" lines in the matrix that do not appear in the other photos. We (including Watkins and Hobbs) do not know their origin, but think they are not relevant to our problem.

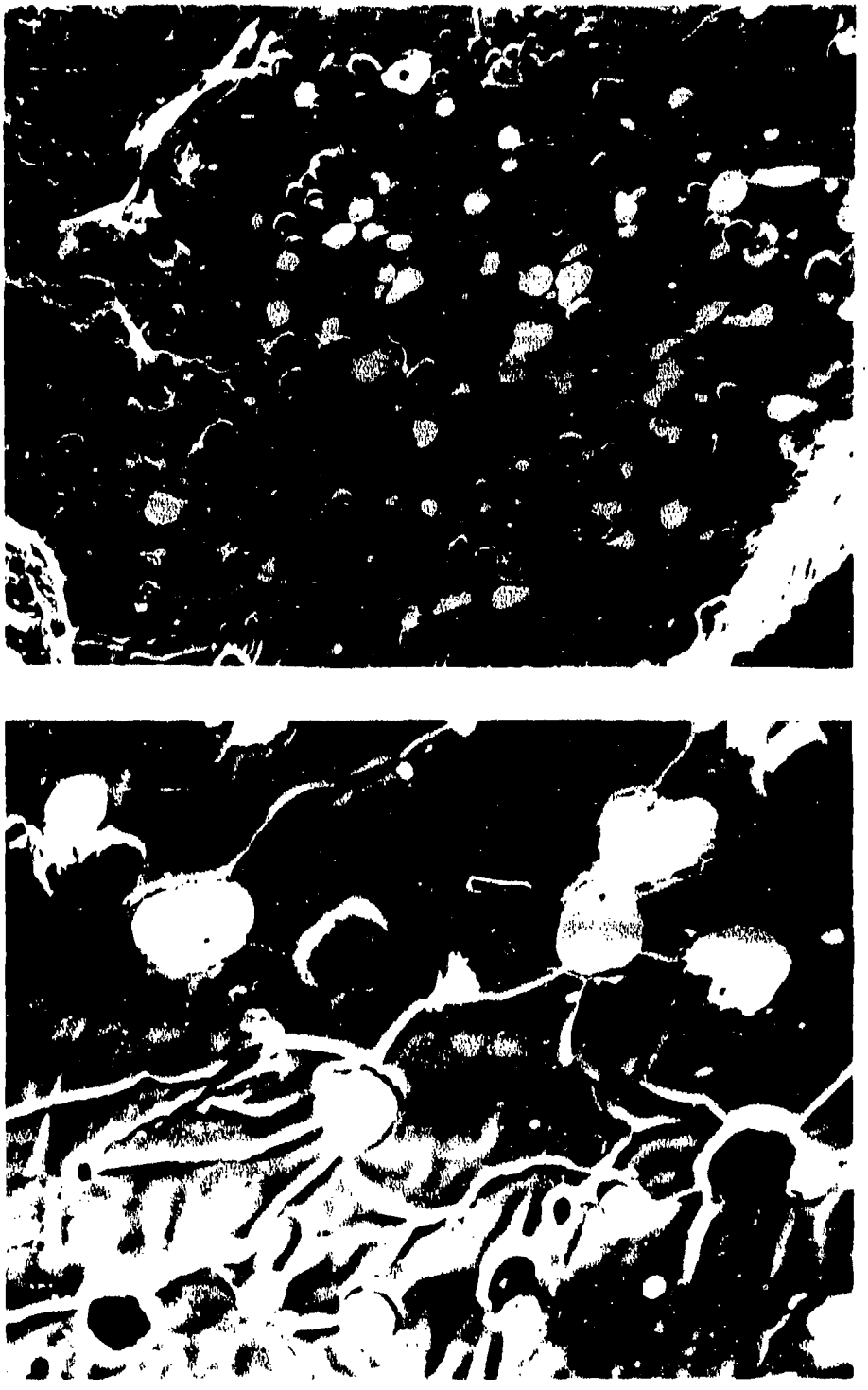

Figure 4a. Scanning electron microscope views of cold-microtomed polymeric composite. Top photo at 150X; lower photo at 500X. ONR No. 5, $p = 0.1$, 20 μm $< d <$ 37 μm.

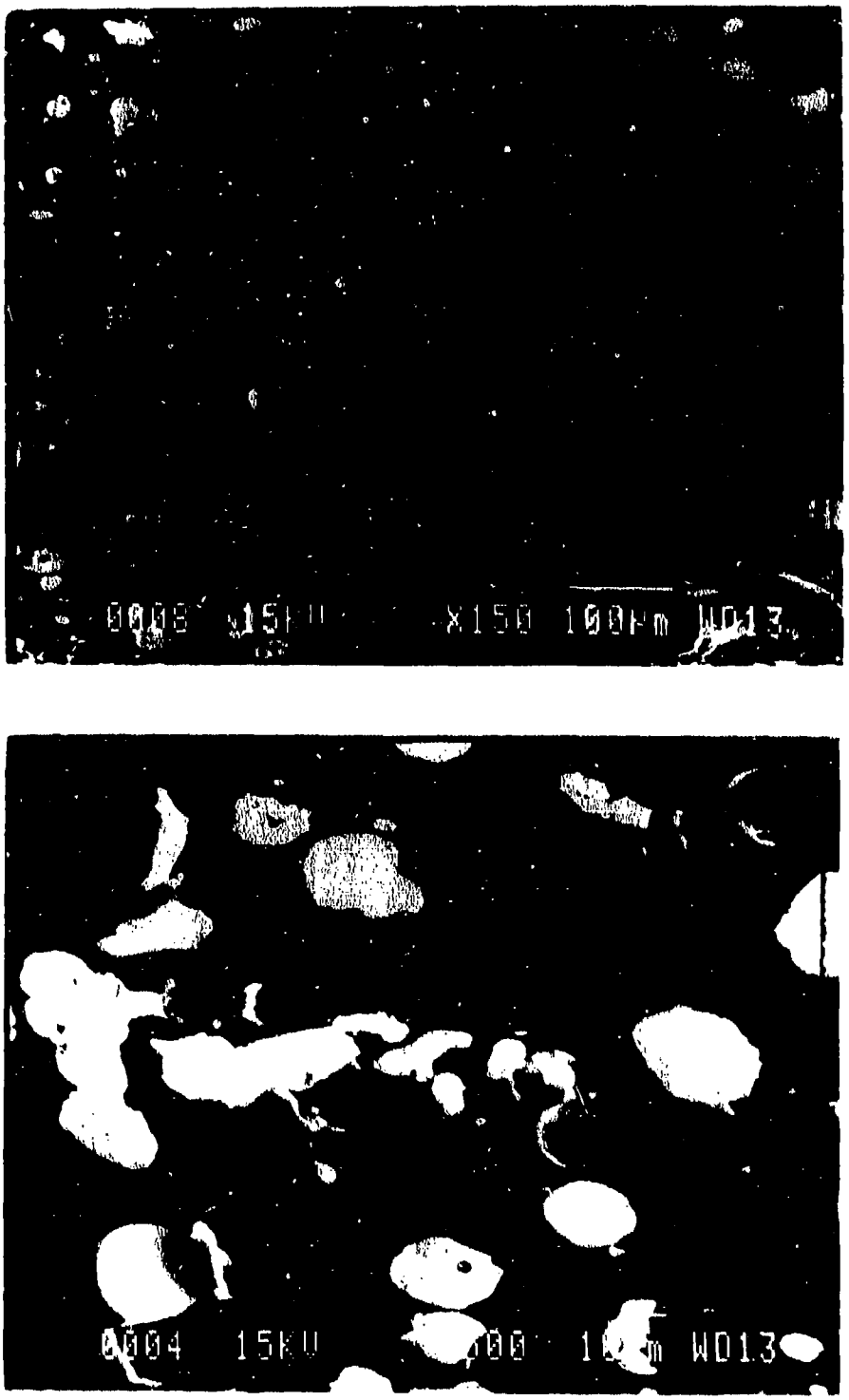

Figure 4b. Scanning electron microscope views of cold-microtomed polymeric composite. Top photo at 150X; lower photo at 500X. ONR No. 4, $p = 0.21$, same d.

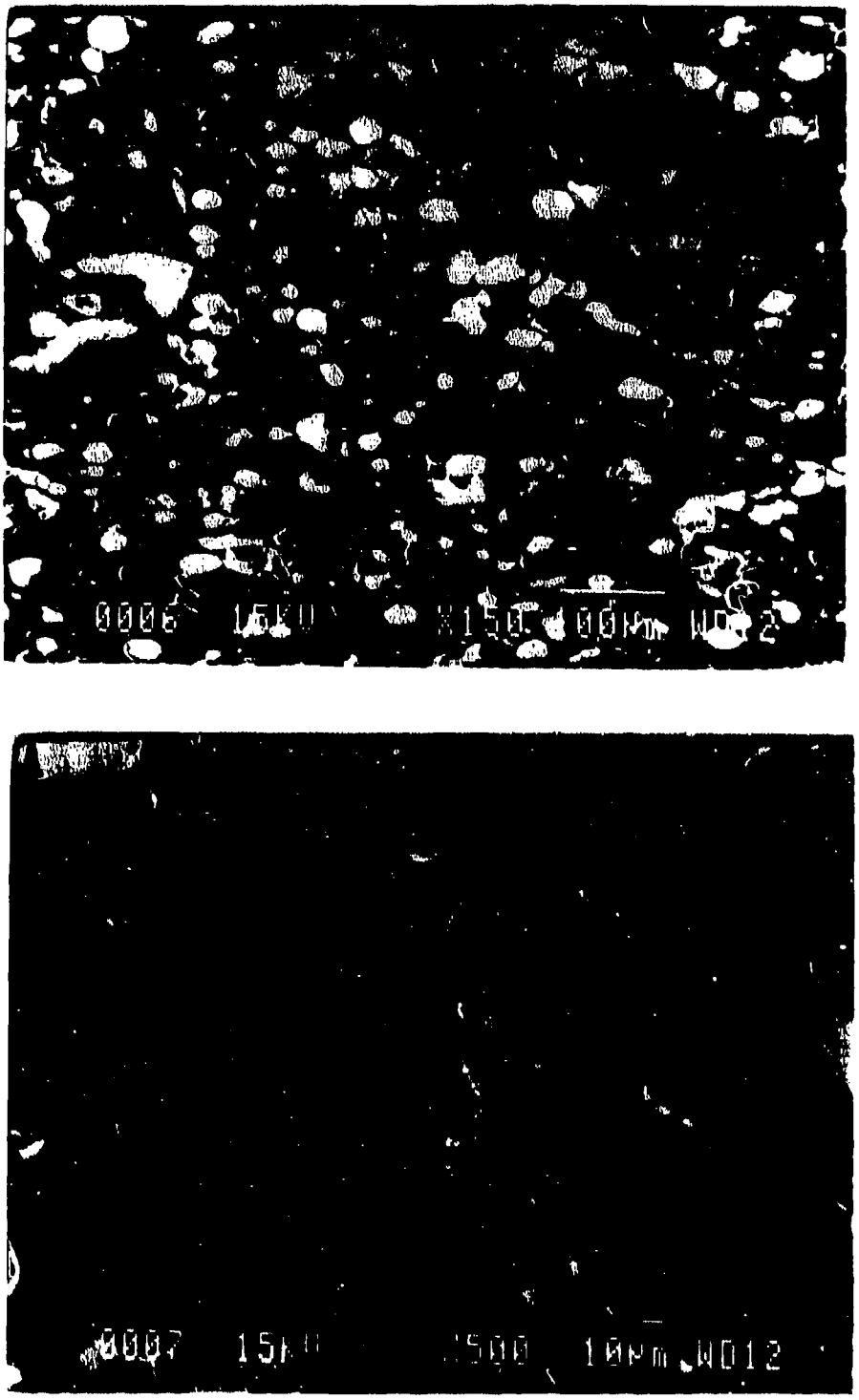

Figure 4c. Scanning electron microscope views of cold-microtomed polymeric composite. Top photo at 150X; lower photo at 500X. ONR No. 3, $p = 0.3$, same d.

II.4 Dielectric Measurements and Analysis

Our prior measurements of the constitutive parameters in the 6 to 12-GHz range of frequency yielded reasonable complex permeability values but some less than ideal results for permittivity (see Figure 34 of Reference 2). For the lower volume loadings, e.g., $p = 0.1$, 0.2, the measurement results for ϵ_r' appeared to be too large by about 50%. This was most obvious when displaying ϵ' versus p, in that there was not an asymptotic trend to the $p = 0$ value for binder alone. When measurements were repeated on newly cut toroids and extended into the 12 to 18-GHz band, there was very little improvement of the results as judged by the expected trends. Suggested explanations based on clumping of the powder did not seem very plausible at these lower volume loadings.

By fortunate contrast, the slotted-line, single frequency measurements at 35 GHz produced results that generally conformed to more reasonable behavior. Even here, some data sets were unacceptable when physically meaningless negative values (of non-negligible magnitude) turned up in computing complex μ and ϵ. Values of ϵ'' are expected to be negligibly small in this system, while values of μ'' may be small, although perhaps not very small. Thus the larger, real quantities may be nearly correct, even when the imaginary components are less reliable but not outlandishly so.

For ϵ_r', repeated measurements at 35 GHz provided from two to six closely grouped values for each of the seven composite samples of the series. The average values are presented in Figure 5, where a smooth departure from the binder-only value is noted. Note also the marked upward deviation from the Mitoff approximation [7] line, which is a simplification of the Maxwell/Clausius-Mossotti calculation for a heterogeneous system whose second phase intrinsic property exceeds that of the host by several orders of magnitude. The Mitoff line is a good representation of the Maxwell calculation out to around $p = 0.5$. The more modern theories, which include higher-order multipole interactions and also consider packing limits more sensibly [8,9,10], do predict more pronounced upward deviations. (See, for example, Reference 2.) This point is examined below.

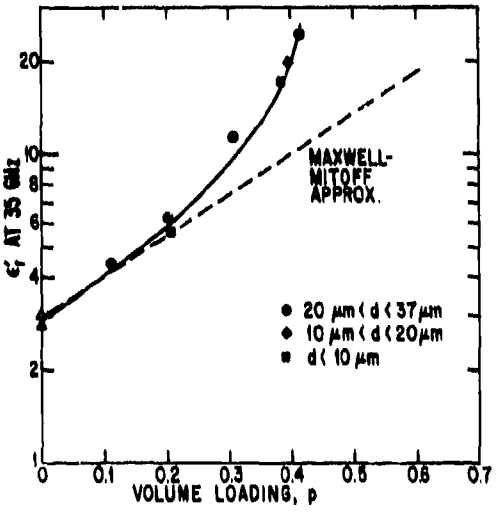

Figure 5. Relative permittivity, ϵ_r', versus volume loading, p, at 35 GHz. Various particle sizes; $Ni_{92}Cr_8$ in polyurethane composites.

Before leaving this sample series, we complete the data presentation by showing in Figure 6 the lower frequency (network analyzer) results, repeated from Figure 34 of Reference 2 (our prior report), with the addition of some 15 GHz data. The defects noted above are obvious. The dotted line represents the experimental curve obtained for the 35 GHz measurements. It remains unclear why only the high volume loading samples give results that are in accord for the two methods. A suggestion that the method works best for higher loss samples is vitiated by the fact that satisfactory results were obtained for the low-loss polymeric binder.

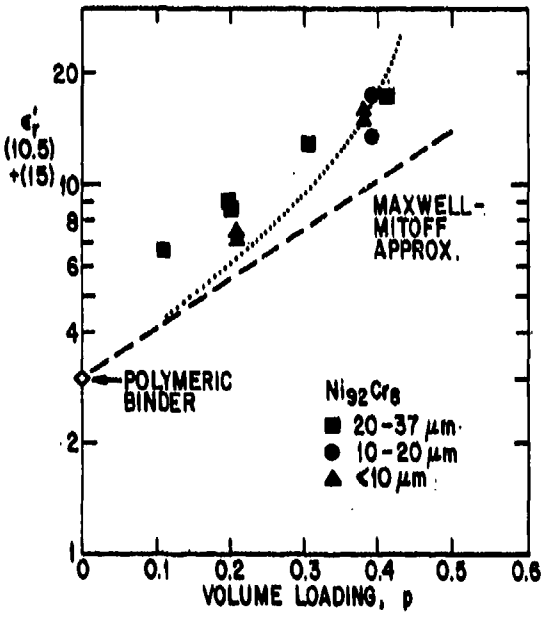

Figure 6. Relative permittivity, ϵ'_r, versus volume loading, on $Ni_{92}Cr_8$/polyurethane composites. Data at 10.5 and 15 GHz from network analyzer, with various particle sizes. Dotted line shows course of data measured at 35 GHz by slotted-line technique (from Figure 5).

The added insight into the ϵ' versus p behavior just described stimulates a re-examination of our earlier series of data on a composite system of magnetic metal particles in polyurethane [1]. (We call this the B-series.) The particles had an insulating coating and the composites had measured volume loadings ranging from about $p = 0.25$ to $p = 0.50$. In our prior analyses [1, Figure 32 of Reference 2], we were so infatuated by the potential of the Maxwell-Mitoff approximation line that we used the line fitted to the lower p-values of the data set (not really very low!). In the limit of $p = 0$, this line (of predetermined slope) came close to, but still deviated a bit from, the separately measured binder value, ϵ'_b. In the greater wisdom of hindsight, we now fix our line and the empirical curve to originate at the binder value as shown in Figure 7. (Note that the different symbols used for the B-series data set refer to sample groups with different particle sizes and size ranges). Most, but not all, of the groups have data that are approximated by the solid line drawn as a guide to the eye. One group falls somewhat below the rest, but still slightly above the Maxwell-Mitoff line. That group has the widest range of particle sizes of the set, about a factor of four from largest diameter to smallest. We conclude from

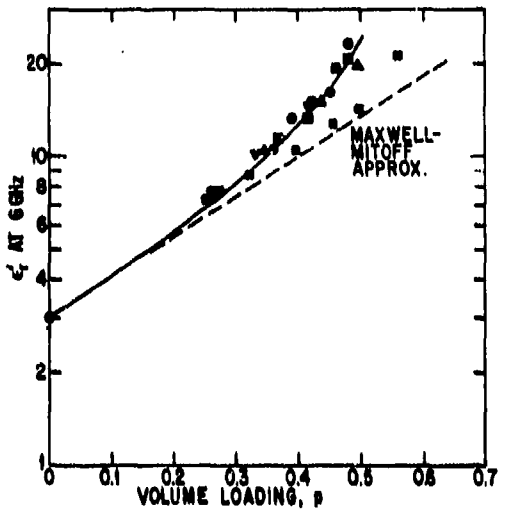

Figure 7. Relative permittivity, ϵ'_r, versus volume loading, p, for B-Series composites. Data from Reference 1.

these presentations of ϵ' versus p data that upward deviations from the Clausius-Mossotti (Maxwell-Mitoff) models occur at lower values of volume loading, p, than suspected in our earlier reports.

Finally, we offer a comparison of these two experimental representations with some of the better theoretical models available. This is shown in Figure 8, where the dashed lines portray the experimental behaviors of the Ni-Cr series (Figure 5) and the B-series, and the series of data points refer to the unusual B-series group. All are plotted as a ratio to the binder ϵ'_b value. One comparison is to the predicted behavior for a simple cubic array (S.C.) calculated on a rigorous model [8,9] which is the array diverging at the lowest p-value ($p = 0.523$). The second comparison is to the quasi-empirical, quasi-theoretical model for a nonpercolating random composite [10]. This idealized random model was constructed to diverge at the empirical packing limit for random systems, $p \cong 0.63$, and fit to a logarithmic divergence which appears to describe the rigorously calculated array models.

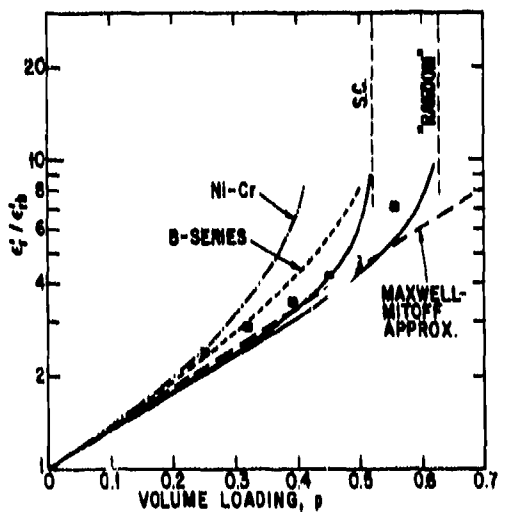

Figure 8. Comparison of experimental studies of ϵ'_r versus p for random composites with some theoretical models.

As noted in our prior report [2] and more solidly reinforced here, the upward curvatures of the experimental sets mimic the theoretical models but precede their predictions noticeably. Professor Doyle has remarked that this could be a natural consequence of localized clumping (higher local volume loading) combined with marked nonlinearity of the ϵ' versus p curves. (Note: Our use of semilogarithmic coordinate paper hides some of the nonlinearity.) We hope to be able to quantify this conjecture in the coming research period by combining microstructural studies such as in Figure 4 with mathematical modeling.

II.5 High-Frequency Permeability Measurements

At the inception of this research program, permeability measurements were not envisaged. However, during the first year [2] it was quickly realized that purely electric dipole phenomena would not suffice to describe fully the high-frequency response of artificial dielectrics. Following the lead of those studying ultrafine particle solar and infrared absorbers [11,12] during the past decade, we examined the role of induced magnetic dipole effects. If the diameter of a conducting particle is not negligible compared to the skin depth, there is a classical mechanism for absorption arising from the magnetic field of the incident radiation. In the time-varying magnetic field, there will be an induced eddy current magnetic polarization and an eddy current loss. The effective permeability of the composite artificial dielectric will thus not be unity even though the dc permeability of the constituents may be exactly unity. These magnetic effects are size-dependent while the electric dipole phenomena are not. Indeed, the magnetic contribution dominates for metallic particles above about 50 Å in size!

We calculated the behavior of an isolated conducting sphere and extended this to a composite of such spheres. Using the known conductivity of the Ni-Cr alloy and the dimensions of particle spheres anticipated, we found that the frequencies envisaged in this study comfortably spanned the parameter space for interesting behavior. Measurements in the 6 to 12-GHz range turned out to be in reasonable agreement (better than a factor of 2) with the model calculations. This was of some interest because of many observations of anomalously high absorption in the far-infrared on particles of sizes from about 1 μm down to about 100 Å. The anomalous deviations were often several orders of magnitude.

Recent work [13-15] has demonstrated that separated particles do not show such anomalies. Our system came into this category naturally, because of the deliberate coating procedures used in preparation of the powder. We reported briefly on the initial results at the March 1985 meeting of the American Physical Society [16], which elicited encouraging comments that "Maxwell's equations really do work!" During the current year we extended the previous measurements to higher frequency, and these results are presented in Figures 9-12 for the real part, μ_r', and in Figures 13-16 for the imaginary part, μ_r''. The addition of higher frequency data, in part from other techniques, increases the scatter but does not destroy the rough accord between experiment and calculation.

As the still higher frequency (millimeter wavelengths) results develop, a more formal presentation (journal publication) of the study will be a desirable contribution.

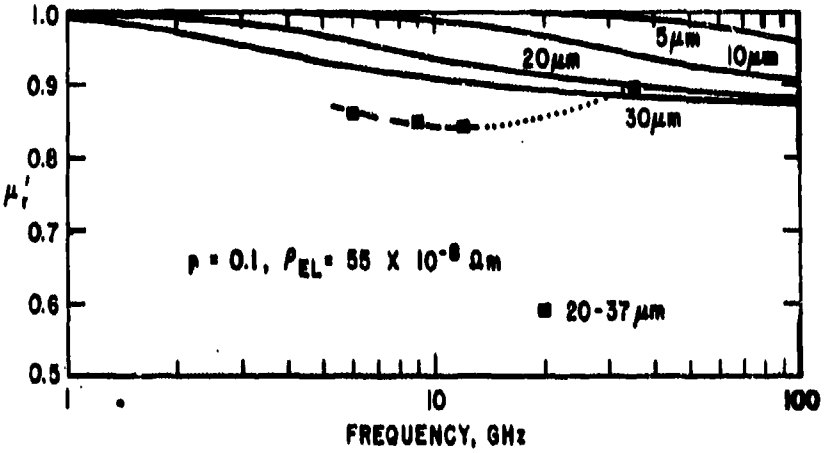

Figure 9. Comparison of experiment and model calculations; μ_r' versus f, p = 0.1.

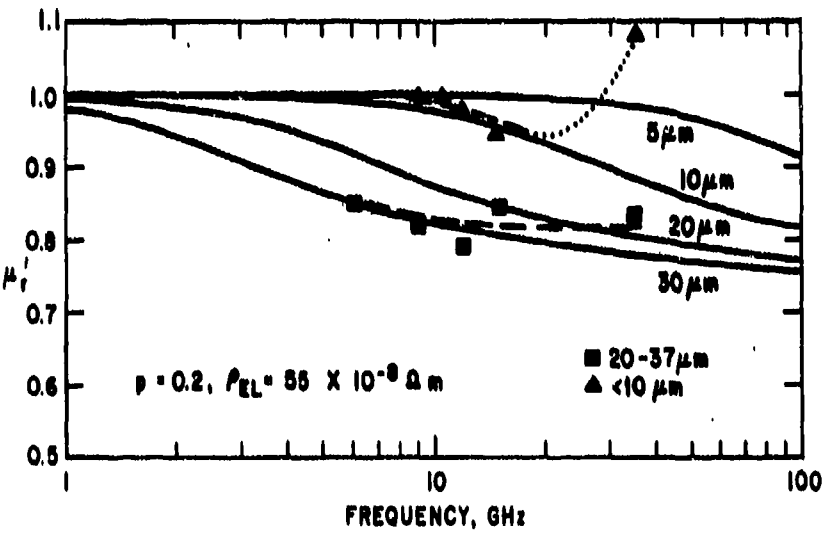

Figure 10. Comparison of experiment and model calculations; μ_r' versus f, p = 0.2.

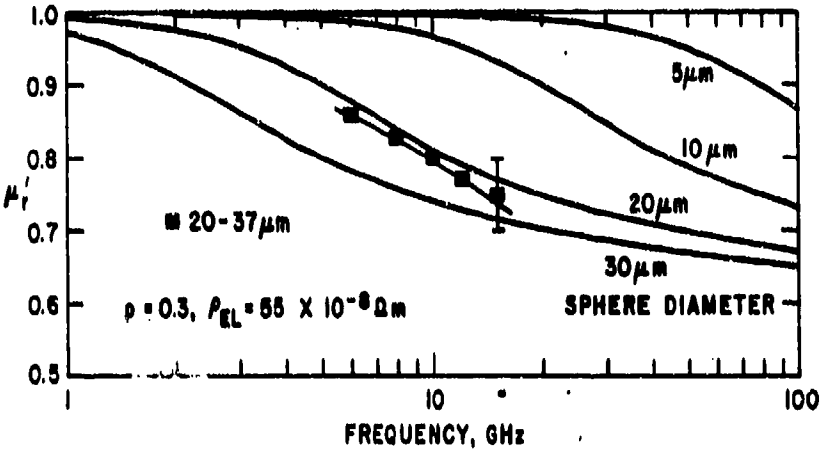

Figure 11. Comparison of experiment and model calculations; μ_r' versus f, p = 0.3.

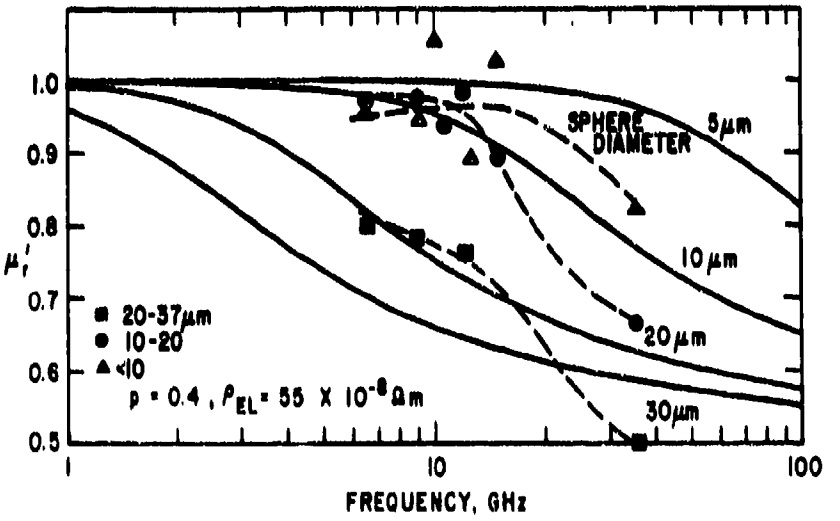

Figure 12. Comparison of experiment and model calculations; μ_r' versus f, p = 0.4.

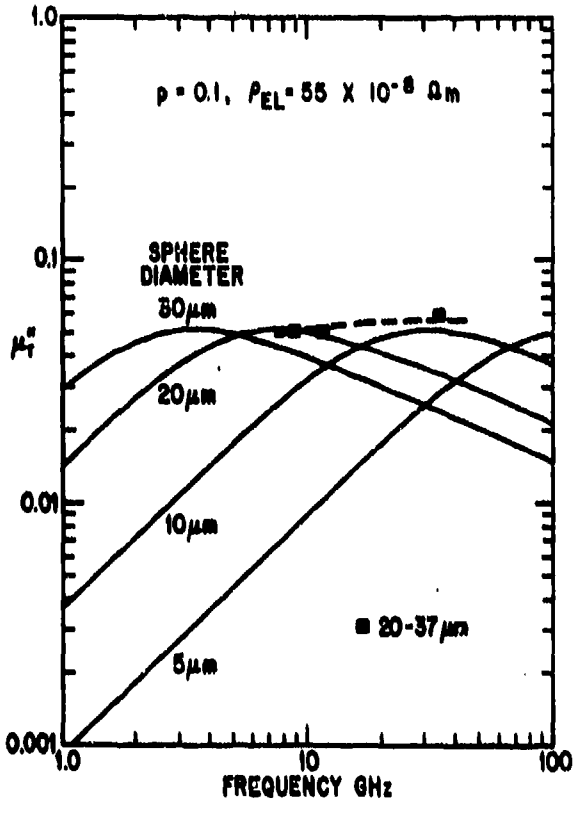

Figure 13. Comparison of experiment and model calculations; μ_r'' versus f, $p = 0.1$.

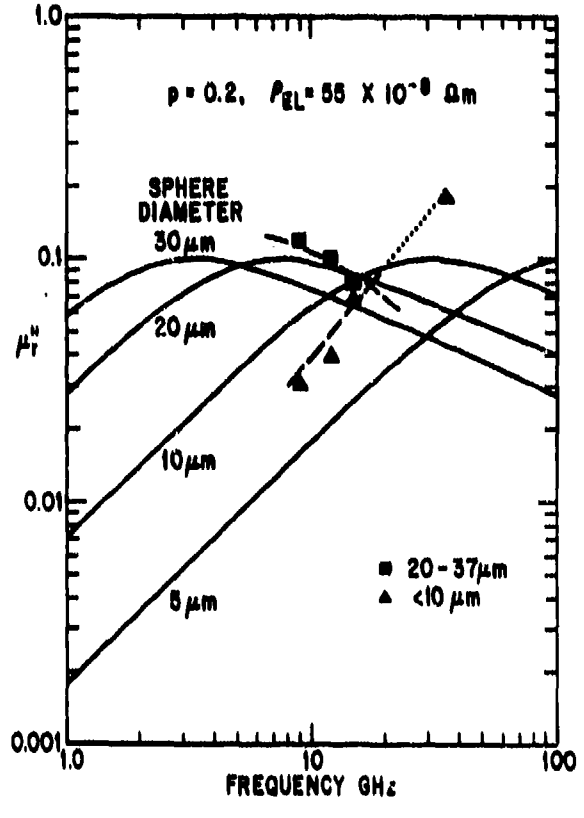

Figure 14. Comparison of experiment and model calculations; μ_r'' versus f, $p = 0.2$.

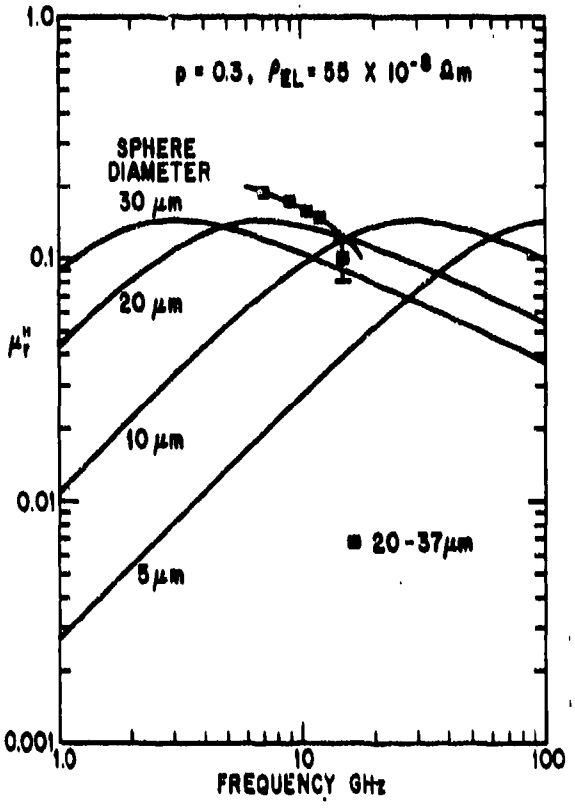

Figure 15. Comparison of experiment and model calculations; μ_r'' versus f, p = 0.3.

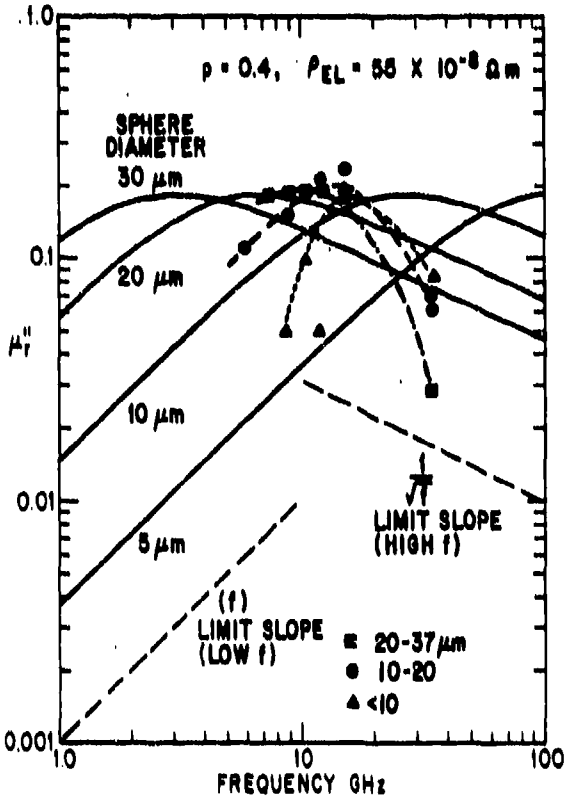

Figure 16. Comparison of experiment and model calculations; μ_r'' versus f, p = 0.4.

III. BINDER PERMITTIVITY EFFECTS

An aspect of the modeling analyses of the permittivity of artificial dielectrics is that the dielectric constant of the binder "sets the level" for the dielectric constant of the composite, and in a multiplicative way. This can be expressed quite simply by citing the formula for the Mitoff approximation to the Maxwell (Clausius-Mossotti) formula, i.e.:

$$\log \epsilon_c' \cong \log \epsilon_b' + Gp$$

or

$$\epsilon_c'/\epsilon_b' \cong 10^{Gp},$$

where c and b represent composite and binder, p is the volume loading of the metal or alloy particles (phase a), and G is a constant of value 1.3. Thus choosing a binder with twice or half the value for ϵ_b' will produce a doubling or halving in the value of ϵ_c'.

The relevance of this effect lies in the effect of ϵ_c' on the wavelength of the electromagnetic radiation *in* the medium, by the formula given in Section II.2. Since electromagnetic applications configurations often are designed with materials of thickness measured in units of the wavelength, the choice of binder could influence the overall weight of the configuration.

In the original proposal one of the tasks was to verify this prediction for artificial dielectrics in the microwave and/or millimeter wavelength regions by comparing composites with two different insulating binders. We proposed that one would be a polymeric binder (many of which have $\epsilon_b' \cong 3$) and that the other would be inorganic (a choice which often means $\epsilon_b' \sim 6$ to 10). The polymeric binder route has been rather straightforward. However, our prior attempts to develop a suitable inorganic binder host reported last year [2] were quite unsuccessful with the alloy system of present interest to us.

We report below on the continuing search for an alternative inorganic binder. The search appears to be close to success, although high frequency measurement samples have yet to be fabricated.

III.1 Search for Alternative Inorganic Binder

At the outset it is useful to enumerate the requirements of the proposed search. The material and process should maintain the shape (usually spherical) of the alloy particles, they should maintain the essential chemical integrity of the alloy, although some small deviation is permitted, and they should maintain a condition of electrical isolation of the particles. Beyond these requirements, the resulting product should have sufficient mechanical integrity to permit machining into high-frequency measurement specimens. Even with the last requirement, there are options in that precision coaxial samples for the microwave (X-) band network analyzer are more demanding of machinability than the thin, solid disks needed for the 35-GHz, slotted-line measurement. We describe below the steps of our current search, as carried out by our collaborators M.B. Borom and L.E. Szala.

Specimens were compounded from a three-component system — paramagnetic Ni-Cr alloy particles as the active component, a choice of two different glasses as the binder, and alumina as an inert filler. Ni-Cr alloy particles of two different particle sizes were used in volume fractions ranging from 15 to 30 vol%. Alumina as an inert, refractory, fine-grained, dielectric material was chosen to keep the metallic particles isolated from one another. Good, high-temperature compressive strength of the alumina contributes to maintaining spacing of the deformable metallic phase, particularly during sintering or hot pressing. The third component to be considered is the binder. (Electrically, all the

nonmetallic components make up the binder, but we are speaking here in the ceramic processing sense). The binder must be sufficiently fluid during processing to flow between the Al_2O_3 and the alloy and create a mechanically strong structure. The binder must flow at a temperature below the melting point of the Ni-Cr alloy, and must also be nonreactive to it. Many glasses with reasonable softening points fit these requirements. Two types of glass were tried: a soda/lime window glass composition designated as Corning code 0800, and a lead-bearing, Owens-Illinois solder glass designated as SG-7. Both glasses have softening points below the melting point of the Ni-Cr alloy.

Powder preparation was accomplished by milling the components in polyethylene jars using 1/4-inch alumina spheres as the grinding material. The alumina, 0.3 μm in size, and the glass were initially wet-milled together in alcohol for 8 to 10 hours to reduce the particle size of the glass and to ensure proper blending of the two components. After the addition of the alloy powder, an additional 1 to 2 hours of milling was performed to disperse the alloy powder. Milling times after the addition of alloy were kept short to prevent erosion of the oxide coating already present on the alloy powder particles. The blended powders were then dried in a rotating evaporator to keep the relatively coarse-grained Ni-Cr in suspension. The dried blends were compacted using standard die and/or isostatic pressing.

Before describing the experiments, we show some SEM photographs in Figure 17 of the Ni-Cr powder from preparation run RS-67, for two powder particle size ranges, as classified. In each case there are a number of rather smaller particles than called for in the nominal range, but they do not represent a significant weight of volume fraction of the bath. The other feature of note is the occurence of some elongated particles among the majority of spherical ones. This is more pronounced in the fraction with larger sizes. At present, we have to live with this, but this fact is important to know, both as a reference and as a possible perturbation on the interpretation of data.

Table 2 is a summary of experiments and results. The table is made up of two sections, with the type of glass used being the prominent variable. Samples are listed alphabetically in each section. The major sections are then divided into segments detailing composition and process variables and results.

Sample 0800-A, a blend of 35% Al_2O_3, 35% 0800 soda/lime glass, and 30% 20-37 μm Ni-Cr powder, was consolidated by hot pressing at a temperature of 950 °C and 600 psi loading. The resultant material shown in Figure 18 appears to meet the requirements of paramagnetism (i.e., not attracted by a small permanent magnet) and is nonconductive; however, the compact has very low strength.

In an attempt to overcome the low strength problems associated with sample 0800-A, a higher hot pressing temperature and loading was employed. It was felt that increasing the temperature to 1300 °C and the pressure to 1200 psi would require a more rigid, less deformable composition. This Ni-Cr content was kept at 30 vol%, while the glass content was decreased to only 10%, and the difference made up by alumina (sample 0800-B). As anticipated, use of higher temperatures and pressures corrected the low strength problem associated with sample 0800-A, but created a problem of its own. Because of the elevated temperature and pressure, the alloy became more deformable and sintered into an interconnected network, thus becoming electrically conductive.

Sample 0800-C was prepared keeping the ratio of Al_2O_3 to glass the same as in 0800-B, but reducing the metallic alloy loading to one half the value, i.e., 15%. Hot-pressing conditions were identical to 0800-B. These conditions produced a very dense, paramagnetic,

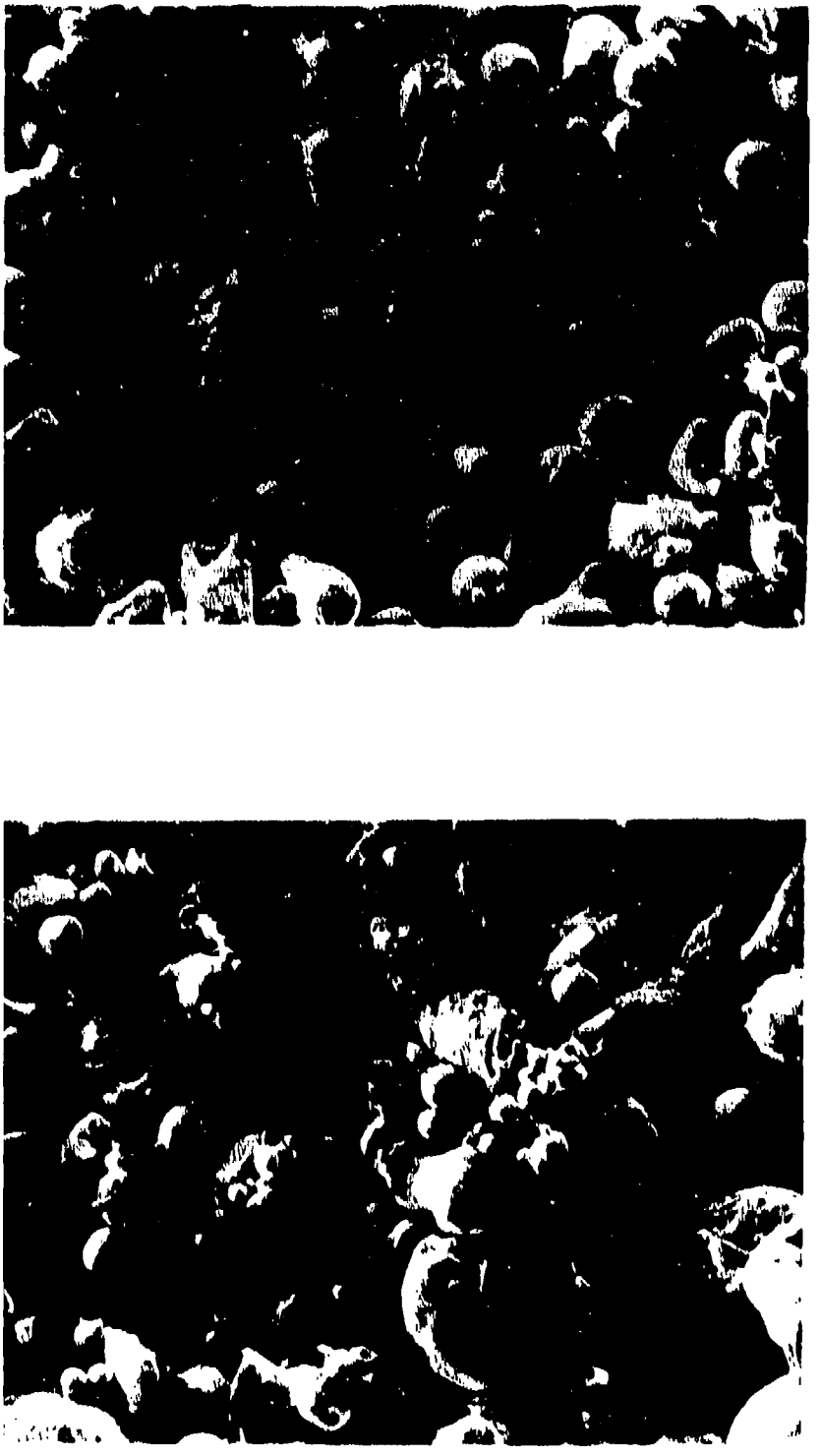

Figure 17. Scanning electron micrographs of Ni-Cr alloy powders from gas atomization preparation run RS-67. Magnification: 1000X. Top photo, nominal 10 μ < d < 20 μm; bottom photo, nominal 20 μm < d < 37 μm.

Table 2

SUMMARY OF PREPARATION EXPERIMENTS IN SEARCH OF SUITABLE INORGANIC HOST COMPOSITE

Sample Ident.	Composition Variables: Matrix: Glass Comp.	Glass v/o	Inert Phase Al_2O_3	Inert Phase v/o	Ratio Inert/Glass	Binder Inert + Glass v/o	Active Particle: Conc v/o	Particle Size (μm)	Comp.	Process Variables: Hot-Press: P (psi)	T_{max} (°C)	t_{min}	Sintering: T_{max} (°C)	t_{min}	Results: Magnetic: Yes	No	Electrically Cond.: Yes	No	Comments
0800-A HP-26-85	0800 Soda/Lime	35	"	35	1:1	70	30	20-37	NiCr	600	950	2				X		X	Mechanically weak
0800-B HP-23-85		10	"	60	6:1	70	30	20-37	NiCr	1200	1300	2					X		Very dense microstructure
0800-C HP-25-85		12.5	"	72.5	6:1	85	15	20-37	NiCr	1200	1300	2				X		X	
0800-D HP-28-85		10	"	60	6:1	70	30	<10	NiCr	1200	1300	2				X	X		
0800-E 5-16-85A		10	"	60	6:1	70	30	<10	NiCr				1000	5	X			X	Compact pre-oxidized to 80
0800-F 5-16-85B		10	"	60	6:1	70	30	<10	NiCr				1000	5	X			X	No pre-oxidation
SG-7-A HP-30-85	SG-7 Lead-Bearing Solder Glass	21	"	79	4:1	100	0	--	--	700	690	2			NA		NA		
SG-7-B HP-31-85		20	"	50	2.5:1	70	30	20-37	NiCr	400	840	2				X		X	
SG-7-C 6-11-85		20	"	50	2.5:1	70	30	20-37	NiCr				1000	5	X			X	Very weak mechanically
SG-7-D 6-28-85		70	--	0	0	70	30	20-37	NiCr				1000	5	X		X		Good strength, Blow holes present
SG-7-E 7-17-85		70	--	0	0	70	30	20-37	NiCr				625	20		X		X	Potential candidate material

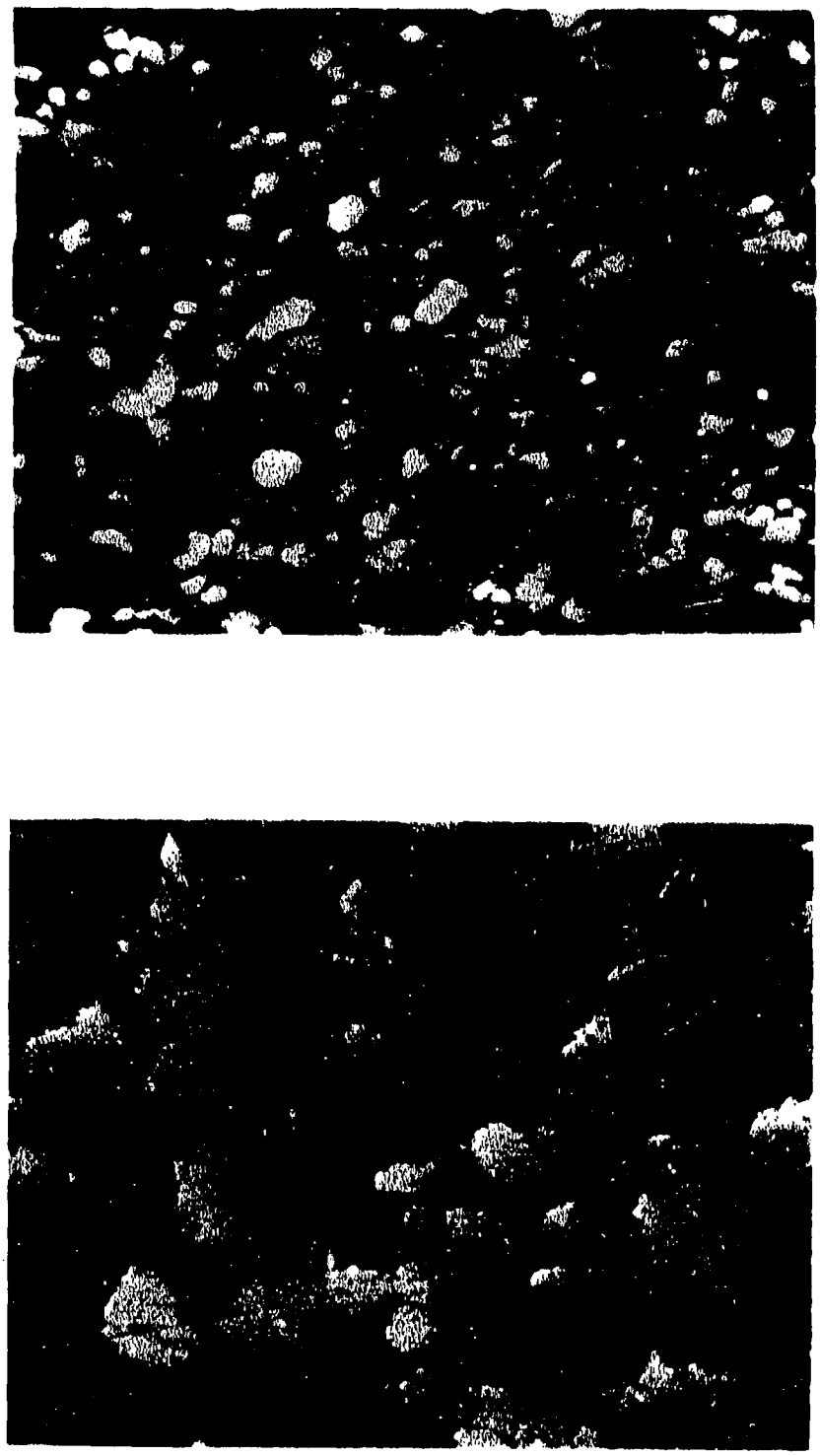

Figure 18. Optical micrographs of inorganic composite sample 0800-A, with soda-lime glass. Preparation parameters given in Table 2. Magnifications at 200X and 500X.

nonconductive sample. The process, however, would probably not be suitable because of the low loading of Ni-Cr alloy.

Sample 0800-D differs from sample 0800-B only in that the alloy particle size was reduced from 20-37 to $<10\,\mu m$. Composition and processing are the same. A smaller particle size was used in an attempt to increase the loading back to 30% and to achieve a better dispersion of the Ni-Cr alloy throughout the mixture, thus possibly creating less contact between the individual particles. It is very difficult to suspend large particles of a dense material in a fine dispersion of a low-density material. Results of the test were poor. Even though the uniformity of the dispersion of Ni-Cr alloy was greatly increased, the material is highly conductive. The result is shown in Figure 19.

The Ni-Cr alloy powder appears to be too deformable at elevated temperatures to withstand unidirectional pressure of hot pressing. Pressure exerted on the system deforms the spherical metal particles into platelets and increases the chance of contacting and sintering together. Therefore, experiments employing pressureless sintering were designed in an attempt to solve the problem of metal-metal contact during consolidation.

Samples 0800-E and 0800-F were compositionally the same as 0800-D (60% Al_2O_3, 30% Ni-Cr ($<10\,\mu m$), 10% 0800 glass). The mixtures were isostatically pressed into 1/2-inch diameter × 5/8-inch long pellets at a pressure of 55 kpsi. In an effort to increase the oxide film thickness on the Ni-Cr particles to assist in preventing metal-metal contact, sample 0800-E was subjected to a preoxidation step by firing the sample to 800 °C in air and holding for 10 min. Both samples 0800-E and 0800-F were sintered in helium at ~50 °C/min to 1000 °C and held at temperature for 5 min. Even though both samples remained electrically nonconductive, the paramagnetic properties of each sample were destroyed. The loss of paramagnetism and development of ferromagnetism was indicated by the ease with which the sample could be picked up and held by a small permanent magnet. Loss of paramagnetic properties was not observed in any of the hot-pressed samples. The change in magnetic properties indicates that the Ni-Cr alloy had been changed compositionally, most likely due to oxidation during sintering and/or preoxidation.

From both the sintering and hot-pressing experiments it became apparent that temperatures in excess of ~900 °C could be detrimental to the Ni-Cr alloy particles both chemically as well as physically. To reduce the processing temperature below 900 °C, a lower softening point glass was selected. The glass selected was a lead-bearing solder glass designated SG-7, which has a working temperature of approximately 600-700 °C.

Sample SG-7A, a mixture of 79% Al_2O_3 and 21% SG-7 containing no metal particles was hot pressed under a static load of 700 psi. The sample completely densified at 690 °C.

Sample SG-7B was formulated with 30% Ni-Cr (20-37 μm). The volume percent of SG-7 was kept at the same level as in SG-7A (20%) and the balance was alumina. The mixture was hot-pressed under a static load of 400 psi. In contrast to sample SG-7A, which glassified at 690 °C, no movement of the press rams occurred until 750 °C. The final pressing temperature was 840 °C. Both the reduced pressure on the sample and the presence of the coarse metal particles probably contributed to the need for higher processing temperature. Density of the resultant compact was excellent. The material was nonconductive and maintained its paramagnetic properties, but as in hot-press experiments the alloy was no longer spherical.

With further evidence that hot-pressing, even at 850 °C, deforms the Ni-Cr alloy particles, sintering was again employed. Sample SG-7C is compositionally identical to SG-7B. The material was sintered at a temperature of 1000 °C for 5 min in 1 atm of helium. The

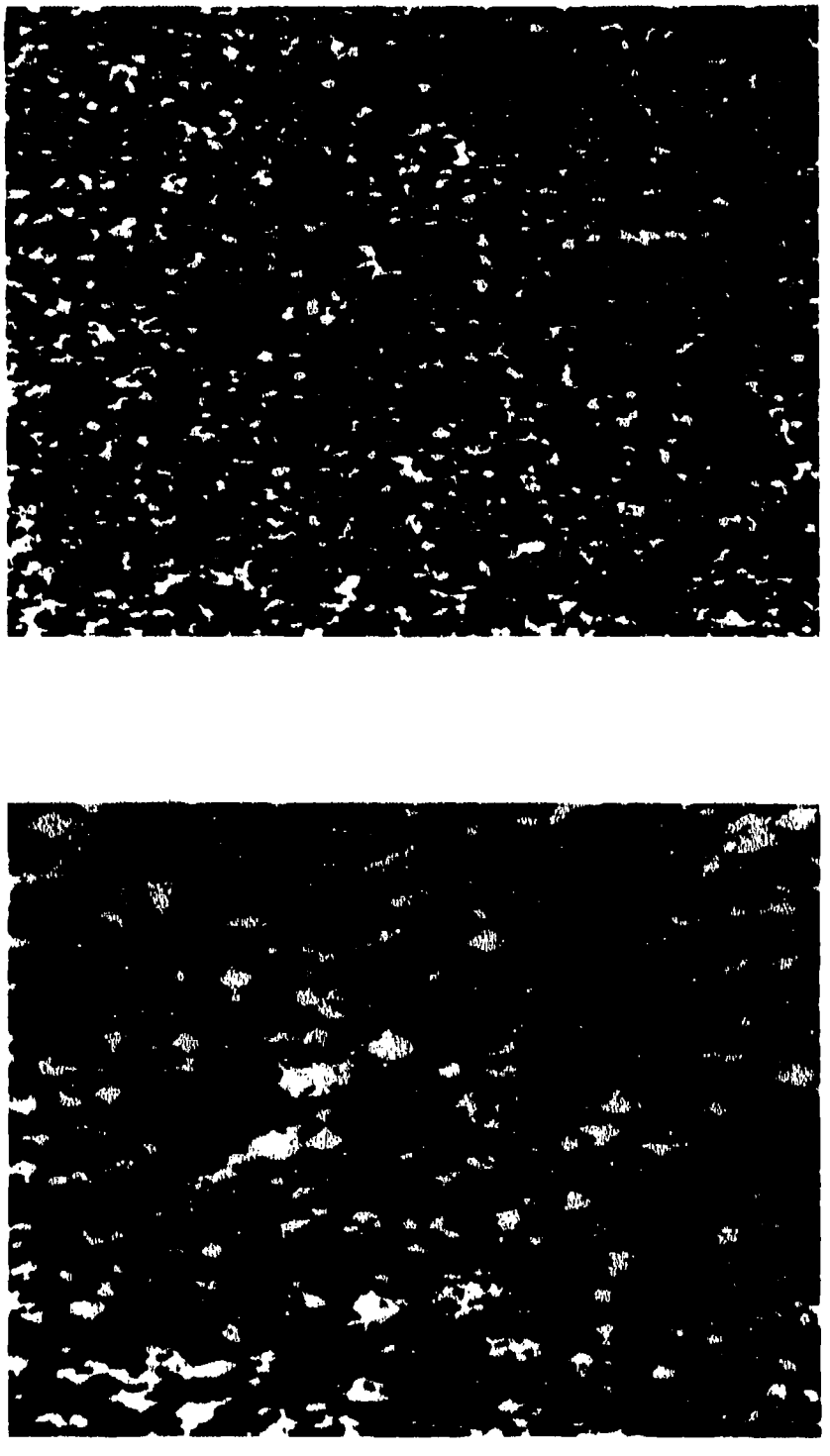

Figure 19. Micrographs of inorganic composite sample 0800-D, with soda-lime glass. Preparation parameters given in Table 2. Magnifications at 200X and 500X.

high temperature was again tried, even though previously unsuccessful, as a direct comparison between the 0800 and the SG-7 glass (via sample 0800-E). The results were nearly the same. The paramagnetic properties were destroyed. The material is nonconductive, but this is primarily because the material is substantially unsintered. A higher content of glass may be required for densification.

After discussions it was decided to relax the potential high-temperature service requirements of the material to see if Ni-Cr could be successfully incorporated in a low-temperature glass matrix without the presence of the refractory alumina phase.

Sample SG-7D is a mixture of 70% SG-7 solder glass and 30% Ni-Cr alloy (20-37 μm). The intent of the experiment was to sinter at ~650 °C, but due to an error in reading a thermocouple scale, the temperature was raised to ~1000 °C. Again, and not surprisingly, the sample failed all the necessary requirements (i.e., it was both ferromagnetic and electrically conductive). Micrographs are shown in Figure 20.

The experiment was then repeated, this time sintering at 625 °C for 20 min. The results (sample SG-7E) were quite encouraging. The paramagnetic and electrical conductivity requirements appear to have been met. Microstructural observations in Figure 21 show the material to be quite dense. The Ni-Cr powder has remained substantially spherical, when compared with its starting state in Figure 17.

III.2 Initial Evaluation Measurements

The procedures used to make sample SG-7E were continued so as to prepare a series of three sample pieces with a range of nominal volume loading (p) values. These were evaluated first by thermomagnetic analysis, similar to that shown in Figure 2, which first verified that the desired characteristic of no ferromagnetism at room temperature was retained, and second, provided data on Curie-temperature and low-temperature (6 K) saturation magnetization from which the actual volume loading could be calculated. The results are presented in Table 3. The Curie temperatures allow one to determine the alloy composition from the data base of our prior report [2]. The saturation magnetization of the Ni-Cr alloy present in the composite follows from the prior data, and when combined with densities of alloy and composite the volume loading is obtained from $p = \sigma_c \rho_c / \sigma_a \rho_a$.

The resulting values are quite acceptable for the nominal 20% and 30% loadings. By contrast, that for the nominal 40% sample is poor. Its low density correlates with a microscopic observation of significant porosity. Another interesting point appears in Table 3: The Curie temperatures are all slightly lower, by 15 to 20 K, than those shown in Figure 2 for the original as-atomized powder. If we assume that there was no sampling problem, nor a significant variation of T_c with particle size, we are led to conclude that a slight reaction did occur in preparing the composite, which shifted the Ni-Cr ratio slightly toward that of the original ingot. It would not impair the application of this material for our purposes.

The other "evaluation" technique attempted was the preparation, by careful machining, of precision coaxial toroids for high frequency measurements. The results were not a success, in that the composites were very brittle and tended to chip or shatter. Where two toroids were needed for measurement at each volume loading, we were lucky to obtain one, and that one might have had small chips at its corners.

We are pursuing experiments on this preparation and we intend to opt for a slightly less demanding machining operation. We shall confine this series to the 35-GHz measurements, which require only a single solid disk for the slotted-line technique. Hopefully this approach will improve the yield.

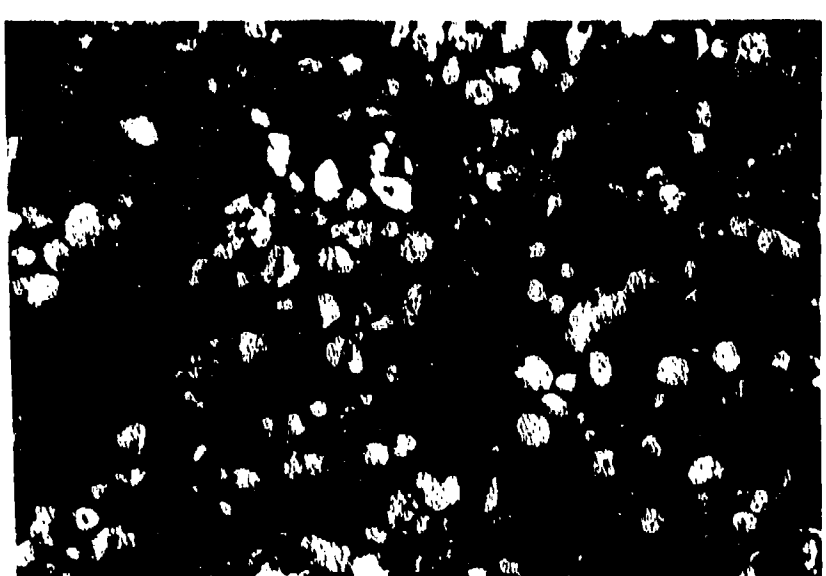

Figure 20. Micrographs of inorganic composite sample SG7-D with lead-solder glass. Preparation parameters given in Table 2. Magnifications at 200X and 500X.

Figure 21. Micrographs of inorganic composite sample SG7-E, with lead-solder glass. Preparation parameters given in Table 2. Magnifications at 100X and 500X.

Table 3

THERMOMAGNETIC EVALUATION PARAMETERS
OF INORGANIC COMPOSITES PREPARED WITH LEAD-SOLDER GLASS
BY LOW TEMPERATURE SINTERING

Sample Ident (Powder Source)	Nominal Alloy (vol%)	Curie Temp.	Sat. Mag. σ_∞ (6 K) (emu/g)	At% Cr	Specific Gravity	Measured Vol Load (p)
SG-7-S (RS-67; $10<d<20$)	20	143 K ±21	5.30	8.2	4.47	0.18
SG-7-E (RS-98; $20<d<37$)	30	137 K ±23	6.75	8.4	5.01	0.27
SG-7-H (RS-67; $10<d<20$)	40	147 K ±26	8.97	8.2	4.23	0.28

IV. CONCLUSIONS AND FUTURE PLANS: PART A

This section summarizes the work of this period related to the subclass of essentially nonmagnetic composite dielectrics, the unclassified portion of the program which has been described in Sections II and III.

IV.1 Conclusions

We have continued our study of the artificial dielectric composites based on a polymeric binder and the alloy powder of $Ni_{92}Cr_8$ prepared by gas-water atomization. We have improved our characterization of the surface condition on the alloy powder particles to demonstrate the presence of an insulating oxide on each particle. We have also obtained micrographs of the polymeric composites at various volume loadings that show the wide variations in local packing density that are characteristic of random loadings.

We have extended the high-frequency measurements of complex permittivity and permeability on these composites up toward 18 GHz with a network analyzer and to a fixed frequency point at 35 GHz using the slotted-line method. Additional samples were prepared for measurements (which are being performed at the Naval Research Laboratory) in the millimeter wavelength regime.

The measurements of permittivity versus volume loading at 35 GHz conform generally to the trend predicted in modern calculations both in a smooth departure from the host binder value and in the upward deviation from the classical Clausius-Mossotti/Maxwell calculation. This extends and improves our evidence for higher-order multipole effects in random systems beyond our prior data on another composite family from AFWAL-TR-82-1040. However, the upward deviation with volume loading is steeper than expected even in the modern theories, for both sets of data. This may be a consequence of clumping, i.e., the observed fluctuations in local packing density as hypothesized last year.

The initial results for the induced microwave permeability were presented publicly and attracted a favorable response. Their significance is heightened because of the connection to a decade-long puzzle over apparently anomalous enhancement of far-infrared absorption by small metal particles. As the millimeter wavelength results develop, a more formal presentation of the results will be a desirable contribution.

To investigate binder permittivity effects, we have been developing an alternative (inorganic) binder with a higher dielectric constant. In processing such a binder with the alloy powder, there are requirements of retaining particle shape and chemical integrity of the alloy, maintaining electrical isolation, and obtaining mechanical integrity for machinability. After a series of experiments with glasses and processes, we believe we have a suitable candidate.

IV.2 Future Plans: Part A

- Complete the fabrication of an artificial dielectric (nonmagnetic) with alternative (inorganic) binder. Carry out enough high-frequency measurements to demonstrate the effect of binder permittivity.
- Investigate the millimeter-wavelength electromagnetic properties of artificial dielectric composites with a polymeric binder, working in collaboration with staff scientists at NRL.
- Endeavor to improve our understanding of the properties of randomly packed artificial dielectrics through a synthesis of theoretical models and experimental results from this work and related studies.

REFERENCES

[1] I.S. Jacobs, H. Kirtchik, J.M. McGrath and R.N. Silz, "Magnetic RAM Technology-Phase II (U)," AFWAL-TR-82-1040, Final Technical Report for Contract F33615-80-C-1040, General Electric Company, Sept. 1982, SECRET.

[2] I.S. Jacobs, "Advanced Artificial Dielectric Materials for Millimeter Wavelength Applications," Annual Technical Report for Contract No. N00014-83-C-0447, Period 1 Aug 83 to 30 Sept 1984, General Electric CRD, Oct. 1984.

[3] S.A. Miller, "Amorphous Metal Powder, Production and Consolidation" in *Amorphous Metallic Alloys*, F.E. Luborsky, ed. (Butterworth, London, 1983) pp. 506-519; S.A. Miller and R.J. Murphy, "A Gas-Water Atomization Process for Producing Amorphous Powders," *Scripta Met. 13*, p. 673 (1979).

[4] See, for example, A.R. von Hippel, *Dielectrics and Waves*, (John Wiley, New York, 1954) p. 71.

[5] K. Hauffe, *Oxidation of Metals*, (Plenum Press, New York, 1965) p. 184, Figure 73.

[6] Y. Saito, T. Inoue, T. Maruyama and T. Amano,"Effect of Oxygen Pressure on the High Temperature Oxidation of Ni-Cr Alloys" in Proceedings of the Third JIM International Symposium, *High Temperature Corrosion of Metals and Alloys*, Transactions of the Japan Institute of Metals, Supplement, pp. 191-198, (1983).

[7] S.P. Mitoff, "Properties Calculations for Heterogeneous Systems" in *Advances in Materials Research*, H. Herman, ed. (Interscience, John Wiley, New York, 1968) vol. 3, pp. 305-329.

[8] W.T. Doyle, "The Clausius-Mossotti Problem for Cubic Arrays of Spheres," *J. Appl. Phys. 49*, pp. 795-797 (1978).

[9] R.C. McPhedran and D.R. McKenzie, "The Conductivity of Lattices of Spheres I. The Simple Cubic Lattice," *Proc. Roy. Soc. Lond. A359*, pp. 45-63 (1978).

[10] D.R. McKenzie, R.C. McPhedran and G.H. Derrick, "The Conductivity of Lattices of Spheres. II. The Body Centred and Face Centred Cubic Lattices," *Proc. Roy. Soc. Lond. A362*, pp. 211-232 (1978).

[11] D.B. Tanner, A.J. Sievers and R.A. Buhrman, "Far-Infrared Absorption in Small Metallic Particles," *Phys. Rev. B11*, pp. 1330-1341 (1975).

[12] A large number of articles and references can be found in *Electrical Transport and Optical Properties of Inhomogeneous Media*, J.C. Garland and D.B. Tanner, ed., AIP Conference Proceedings, No. 40 (American Institute of Physics, New York, 1978).

[13] R.P. Devaty and A.J. Sievers, "Far-Infrared Absorption by Small Metal Particles," *Phys. Rev. Lett. 52*, pp. 1344-47, (1984).

[14] W.A. Curtin and N.W. Ashcroft, "Theory of Far-Infrared Absorption Small-Metal-Particle-Insulator Composites," *Phys. Rev. B31*, pp. 3287-3295 (1985).

[15] S.-I. Lee, T.W. Noh and J.R. Gaines, "Effect of an Oxide Layer on the Far-Infrared Absorption of Small Silver Particles," *Phys. Rev. B32*, pp. 3580-85 (1985).

[16] I.S. Jacobs, S.A. Miller, H.J. Patchen and J.O. Hanson, "Microwave Permeability of Random Metal-Particle Composites," *Bull. Am. Phys. Soc. 30*, p. 308 (1985).